Sensor materials

Soft Tactile Sensors Having Two Channels With Different Slopes for Contact Position and Pressure Estimation

Hirono Ohashi[1,2], Takuto Yasuda[1], Takumi Kawasetsu[1*], and Koh Hosoda[1**]

[1] *Graduate School of Engineering Science, Osaka University, Osaka 560-0044, Japan*
[2] *Department of Agricultural Innovation for Sustainability, Tokyo University of Agriculture, Kanagawa 243-0034, Japan*
[*] *Member, IEEE*
[**] *Senior Member, IEEE*

Manuscript received 28 February 2023; revised 28 March 2023; accepted 7 April 2023. Date of publication 21 April 2023; date of current version 8 May 2023.

Abstract—Tactile information is usually important for object manipulation and grasping. Typically, soft hands and tactile sensors can deform passively and contribute to stable grasping. In particular, soft tactile sensors that use conductive materials as sensor elements can acquire contact information, including the contact position and pressure; however, this tactile information cannot be classified. This study attempts to classify tactile information based on conductive material arrangements. To this end, we develop a soft tactile sensor composed of a silicone rubber body with two channels filled with a conductive material. The two channels are arranged so that they are parallel from the top view and angled with different slopes from the side view. Our experimental data reveal that the contact position parallel to the channels can be determined based on the resistance changes in the two channels, whereas the pressure can be obtained through a model based on the estimated value of the contact position.

Index Terms—Sensor materials, sensor applications, force and tactile sensing, ionic gel, perception for grasping and manipulation, soft sensors.

I. INTRODUCTION

The grasping of objects is an essential task for humanoid robots and industrial arms. Typically, such grasping tasks are based on tactile information obtained through slip detection, object classification [1], [2], shape estimation [3], and object pose estimation [4]. For example, Pirozzi and Natale [4] attached a soft tactile sensor to the surface of a hard robot gripper, and the hard robot gripper could insert a wire into a hole by estimating the contact position, contact pressure, and pose of the grasping wire. Moreover, visual information, as well as tactile information, is used for grasping tasks [5]. When estimating the position of a grasped object, cameras can cause occlusion of the object owing to the hand/gripper, complicating accurate estimations of its position. Thus, tactile information can be effective in grasping tasks, especially estimating the position of grasped objects.

Contact position estimation methods using tactile sensors have been developed. Typically, pressure sensors that are excellent for point measurements are arranged in a grid pattern, and they are used as flexible contact position sensors. Contact position identification is performed by identifying the responding pressure sensors [6], [7], [8]. A method referred to as electrical impedance tomography has also been developed to identify the contact position by arranging conductor channels in silicone in the form of a grid and by measuring the voltage [9]. However, when the measurement range is expanded, both methods require numerous wires to connect the elements to each other and to the sensor and measurement equipment. In addition, the measurement cost is high owing to the need to collect sensor values from numerous sensing elements.

Soft-tactile sensors using conductive materials as sensor elements have been applied to impedance tomography, and various types have been developed [9], [10]. In tactile sensors wherein a pressure-sensitive channel filled with conductive materials (hereafter referred to as a channel) is embedded with an elastic material, the deformation of the channel, that is, the contact information obtained from the sensor, can be determined by measuring the resistance of the channel [11]. In this sensor, the contact information, including the contact pressure and position, is superimposed on the scalar value of resistance, and the values can be discriminated and estimated based on multiple measurements using two or more channels. However, the theoretical equation used to assess the change in resistance resulting from the channel contact is complicated because it considers the complicated deformation of the soft material [12]. Usually, the classification of tactile parameters that cause a change in resistance simultaneously is difficult; these may include the contact pressure or position.

The objective of this study is to develop a soft tactile sensor capable of easily classifying information on the contact position and pressure. In particular, a tactile sensor with a conductive material can change the sensitivity of the sensor and the tactile information obtained depending on the arrangement of the channels. Therefore, we investigate the feasibility of separating the contact position and pressure based on channel design to distinguish between different types of contact information. Thus, in this study, a soft tactile sensor with two channels that were crossed and placed parallel to each other is constructed. With this structure, the contact position along the direction parallel to the channel can be easily estimated based on the ratio of the change in resistance for the two channels, and the pressure could be estimated from the theoretical equation.

II. PROPOSED SOFT TACTILE SENSOR

A. Sensor Structure and Working Principle

Fig. 1(a) presents the proposed sensor with conductive material channels for contact position and pressure estimation. The sensor

Corresponding author: Hirono Ohashi (e-mail: ho208307@nodai.ac.jp).
Associate Editor: G. Langfelder.
Hirono Ohashi and Takuto Yasuda contributed equally to this work.
Digital Object Identifier 10.1109/LSENS.2023.3268888

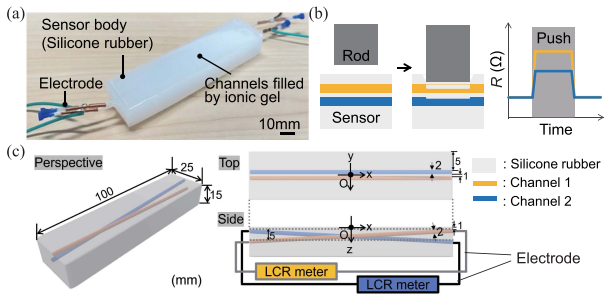

Fig. 1. (a) Overview of the proposed sensor. (b) Working principle of the proposed sensor. (c) Schematic diagram of the proposed sensor.

consists of two channels embedded in silicone rubber, along with a silicone tube and an electrode made of copper pipes. The two channels are arranged in parallel and angled with different slopes [see Fig. 1(c)]. The upper surface of the sensor (x–y plane) represents the contact surface. The sensor body has the following dimensions: width, length, and height of 25, 100, and 15 mm, respectively. The cross-sectional shape of the channels is a square with a side of 2 mm, and the distance between each channel is 1 mm. Each channel is arranged diagonally at a depth of 1 mm at one end and 6 mm at the other end of the channel. These parameters were determined based on data from preliminary experiments.

In particular, ionic gels are conductive polymer gels, and their resistance changes with changes in their cross-sectional area. A contact force applied to an ionic gel channel decreases the cross-sectional area of the channel [see Fig. 1(b)]. Thus, ionic gels can be used as pressure-sensitive sensors based on their resistance. Assuming that the ionic gel channel is pushed from directly above, the resistance of the ionic gel changes, and it (ΔR) can be expressed by the following equation [12]. To simplify the original complicated form of the equation, the equation is expressed separately with χ, c_1, c_2, c_3, and c_4 as follows:

$$\begin{aligned}
\Delta R &= \frac{\rho L}{wh}\left\{\frac{1}{1-\frac{2(1-\nu^2)w\chi p}{Eh}}-1\right\}\\
\chi &= \frac{c_1c_2-c_3}{c_4}\\
c_1 &= 2\tan^{-1}\left(\frac{a}{2z_i}\right)\\
c_2 &= 8z_i^2a^2+16z_i^4+a^4\\
c_3 &= 4z_ia^3+4z_i^3a\\
c_4 &= \pi(a^2+4z_i^2)^2
\end{aligned} \tag{1}$$

where ρ denotes the electrical resistivity, and L and a represent the lengths of the contact object along the parallel and perpendicular directions of the channel, respectively. h and w denote the vertical and horizontal cross-sectional areas of the channel, respectively, ν denotes Poisson's ratio, p is the contact pressure, E is the elastic modulus, and z is the depth from the sensor surface to the ionic gel channel. Based on (1), assuming that the shapes of the contact object, i.e., L and a, remain constant, the resistance change ΔR can be considered as a function of the contact depth and pressure applied to the ionic gel channel.

As stated, in the proposed sensor, the two channels are parallelly and diagonally aligned. Here, the depth of the ith ionic gel channel, z_i, can be expressed using the contact position x as follows:

$$z_i = k_ix + C \tag{2}$$

where k_i ($i = 1, 2$), and C denotes constants that determine the slope and intercept of a channel, respectively. Thus, (1) can be considered as an equation for the contact position and pressure, and the foregoing parameters can be obtained based on the resistance changes in each channel (ΔR_1 and ΔR_2). However, obtaining an analytical solution is difficult, and obtaining a numerical solution is computationally expensive.

Thus, to obtain the solution easily, we can estimate the contact position by clearly calculating the ratio of the resistance changes in the two channels by placing them diagonally across each other [see Fig. 1(b) and (c)]. For example, in the right half of the sensor, channel 1 is closer to the surface of the sensor than channel 2. Thus, when the right-hand side of the sensor is pressed, the change in resistance is greater for channel 1 than that for channel 2 ($\Delta R_1 > \Delta R_2$). By contrast, when the left-hand side of the sensor is pressed, the change in resistance for channel 2 is greater than that for channel 1 ($\Delta R_1 < \Delta R_2$). Therefore, the ratio of the change in resistance for the two channels ($\Delta R_1/\Delta R_2$) increases monotonically from the left-hand side to the right-hand side for the sensor, and the contact position can be obtained simply by calculating this ratio. Therefore, the contact position can be determined based on the ratio of the change in resistance for the two channels. Furthermore, z_i is obtained from (2) using the estimated contact position, and then the pressure can be analytically determined by z_i, ΔR to correspond to z_i, and (1). In our sensor structure, we set the slope k_1, k_2, and intercept C of the channel in (2) to 0.0833, −0.0833, and 3.5 mm, respectively.

B. Fabrication Process of the Ionic Gel Sensor

A 3-D printed plastic mold was used to fabricate the sensor body. A rod with the same shape as the ionic gel channel was fabricated using a water-soluble polyvinyl alcohol (PVA) filament and fixed to the mold. Uncured silicone rubber (Eco-Flex 00-30, Smooth-On, Inc., PA, USA) was then poured into the mold and hardened using a vacuum dryer (AVO-310NB, ETTAS, AS ONE Corp., Japan). The cured silicone rubber was removed from the mold, and hot water was continuously poured onto the PVA rod to dissolve it, consequently creating a channel. Soft silicone rubber tubes with outer and inner diameters of 2 and 1 mm, respectively, were inserted into both ends of the channel and glued to the silicone rubber. As electrodes, copper pipes were embedded into the silicone rubber tube, and a silicone tube was inserted into the other end. Finally, the following uncured ionic gel [1-butyl-3-methylimidazolium bis(trifluoromethanesulfonyl)imide · 1,9-nonamethylene glycol dimethacrylate · pentaerythritol tetrakis] was injected using a syringe, and a Poly-actic Acid (PLA) plug was inserted at both ends of the tube. The ionic gel was cured under ultraviolet irradiation.

C. Indentation Experimental Setup and Method

We conducted experiments to verify the ability of the proposed sensor in estimating the contact position and pressure. A plastic indenter was employed to apply contact pressure. A contact surface of indenter has the following dimensions: width (x-axis) and length (y-axis) of 5 and 25 mm, respectively. This contact surface was sufficiently large to simultaneously push the two channels. The indenter was attached to a triaxis robot stage (TTA-C3-WAW30-25-10B-NP-E-E-2-1, IAI Corp., Japan) to perform the quantitative indentation tests. The ionic gel channel resistance was measured using an *LCR* meter (LCR6200, GW Instek, Taiwan), as shown in Fig. 1(c).

The indenter was pressed while the contact position and depth were changed. The indenter moved along the x-axis from −30 to 30 mm

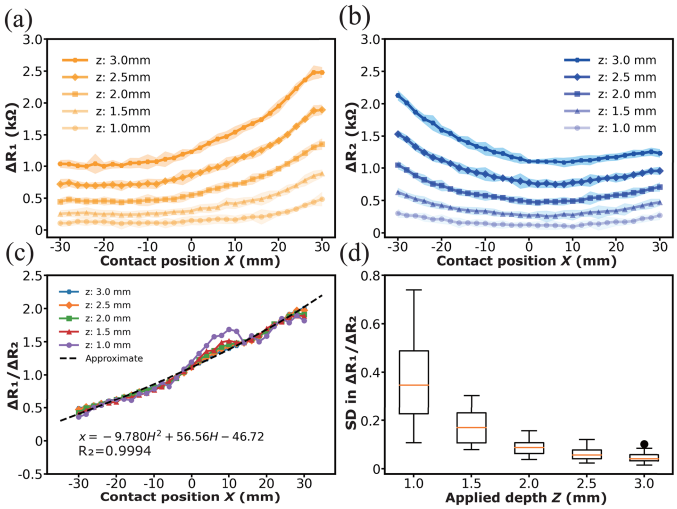

Fig. 2. Change in resistance for (a) channel 1 (ΔR_1) and (b) channel 2 (ΔR_2). (c) Ratio of the change in resistance for the two channels ($\Delta R_1/\Delta R_2$). (d) Standard deviation (SD) of $\Delta R_1/\Delta R_2$.

with an interval of 2 mm. The depth of indentation, z, was varied between 1.0 and 3.0 mm from the top surface of the sensor in steps of 0.5 mm. The applied pressure at each depth was measured 10 times using a digital force gauge (FGP-5, NIDEC-SHIMPO, Corp., Japan), and the mean value was obtained and compared with the estimated contact pressure. The moving speed of the indenter was set to 1 mm/s. Here, we defined the difference between the resistance values under a no-load condition and under pressing as the amount of change in resistance ΔR, and this was measured. Resistance under pressure was measured for 1 s from the 4th second of pressing.

III. RESULTS

The relationship between the contact position (X) and resistance change was investigated under five pushing depth (Z) conditions. Fig. 2(a) and (b) presents the mean (•) and standard deviations (SD, shading) of the resistance change observed in channel 1 and channel 2 (ΔR_1 and ΔR_2), respectively. These data indicate that ΔR_1 and ΔR_2 increased depending on the pushing depth [see Fig. 2(a) and (b)]. ΔR_1 and ΔR_2 at the same pushing depth monotonically decreased and increased, respectively, with the depth of the channel, that is, the contact position. We further investigated if the ratio of the resistance change varied monotonically with the actual contact position. For this, $\Delta R_1/\Delta R_2$ at each contact position is illustrated in Fig. 2(c). The data indicate that the ratio $\Delta R_1/\Delta R_2$ increases monotonically with the contact position, regardless of the pushing depth. The SD of $\Delta R_1/\Delta R_2$ was also found to be greater under conditions of smaller contact depths, particularly 1.0 mm see [Fig. 2(d)]. The contact position was estimated by fitting the ratio of resistance change in two channels using mean values of $\Delta R_1/\Delta R_2$ (H) at each contact position obtained at pushing depths between 1.5 to 3.0 mm [see Fig. 2(c)], using the least-squares method. However, data from the pushing depth of 1.0 mm were excluded from fitting as it would reduce the correlation coefficient value (R^2). The approximate curve is presented by a black dotted line, and the equation and R^2 are presented at the bottom [see Fig. 2(d)]. The fitting results indicate a strong correlation between the contact position and $\Delta R_1/\Delta R_2$.

The fitting results were used to investigate whether the contact position could be estimated based on the obtained $\Delta R_1/\Delta R_2$. The same experimental procedure was used to determine $\Delta R_1/\Delta R_2$, and the contact position was estimated based on the fitting results displayed in Fig. 2(c). The estimated results are illustrated in Fig. 3(a)–(e). Here, the horizontal axis represents the actual contact position (X), and the vertical axis represents the estimated contact position (X'). The circles represent the mean value of X' (mean X'), and the shaded region represents the SD. The black dotted line represents the approximate equation obtained from the mean X', and the equation and correlation coefficient (R^2) are displayed in the upper left-hand corner of each graph. Since R^2 approximates 1, it shows that the X' s are identical to X.

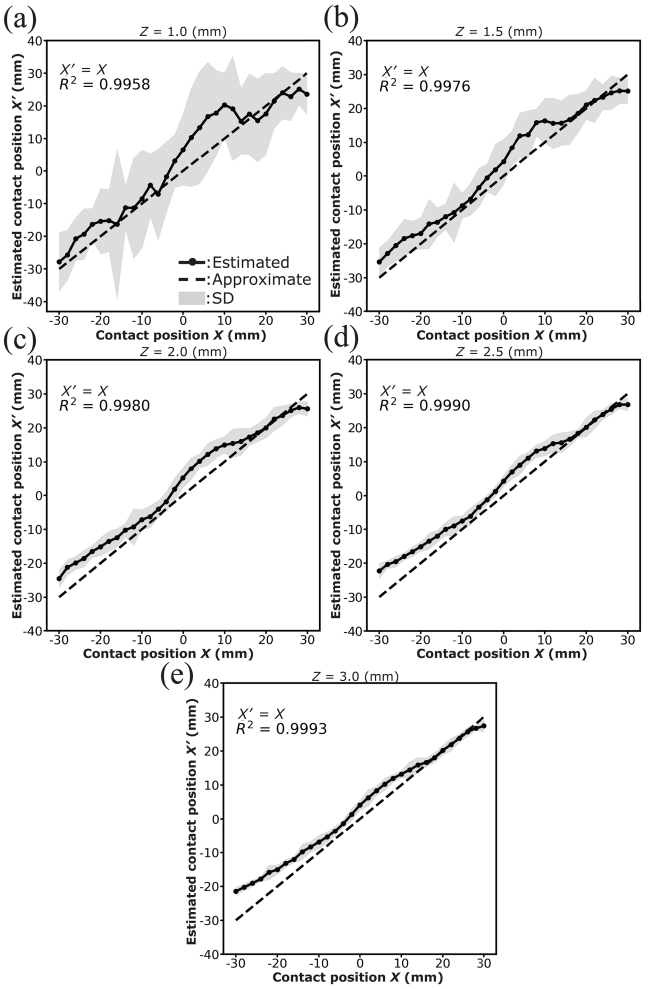

Fig. 3. (a)–(e) Prediction of contact position in each pushing depth.

Furthermore, z_i can be calculated by substituting the contact position into (2), and the contact pressure (p) can be determined by the obtained z_i, ΔR to correspond to z_i, and (1). Estimated contact pressure is shown in Fig. 4. Among all pushing depth conditions, the estimated pressure at the edge of the sensor is higher than the actual value while the estimated one near the center of the sensor is close to the actual value.

IV. DISCUSSION

The ratio of resistance changes for the two channels ($\Delta R_1/\Delta R_2$) increases monotonically with contact position, regardless of pushing depth (see Fig. 2). Thus, the contact position can be estimated by taking $\Delta R_1/\Delta R_2$. The error of the estimated position was 5 mm,

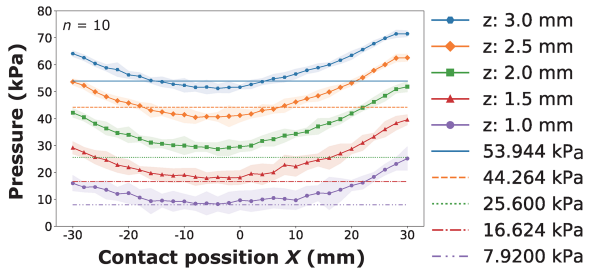

Fig. 4. Estimated contact pressure at each contact position and depth. Each straight line shows the value of the pressure measured at each indentation depth.

which is comparable to the spatial resolution of the human mentum's tactile sense [13], and the maximum error of the contact position was 28 mm when the pushing depth was shallow (see Fig. 3). The reasons for the large estimation error are that the width of the indenter used to create the estimation equation was 5 mm, and the smaller the contact pressure, the greater the effect of noise on the degree of change in resistance value. To solve this problem, the sensor value can be improved by making the indenter smaller. The sensitivity of the sensor will be improved by making the silicone rubber softer and by improving the resistance change of the ionic gel. The proposed sensor can approximately evaluate contact pressure (see Fig. 4), but discrepancies between the estimated and actual contact pressure exist due to the oversimplification of the theoretical equation for the resistance change of ionic gel and the contact position estimation error. To improve the accuracy of contact pressure estimation, the theoretical equation should be modified to account for sources of error, such as surface tension and nonuniform deformation, of the ionic gel channel.

In soft robot applications, it is essential that the contact sensor is sufficiently thin to conform to any given shape. The proposed sensor has a thickness of 15 mm. As the thickness of the sensor is reduced, the slope of the channel decreases, resulting in an insignificant difference between ΔR_1 and ΔR_2. Consequently, position direction detection may become challenging when the sensor is excessively thin. In other words, there is a tradeoff between the required position estimation accuracy and the thickness of the sensor. Future investigations will aim to explore the relationship between the estimation accuracy and the sensor's thickness by grasping experiments.

We investigate the possibility of classifying contact position and pressure based on channel arrangement and demonstrated that the proposed sensor can estimate both. The proposed sensor measures resistance value and has a simple structure for sensor readout parts. It does not require additional sensors or wiring even if the measurement range is extended. This allows for position identification with fewer wires than conventional methods, such as electrical impedance tomography, when a long measurement range is needed in a constant direction. Therefore, the proposed sensor estimate contact position and contact pressure with minimal measurement and calculation costs. The future study aims to develop applications and methods for the accurate estimation of contact position and pressure, and a method to separate contact information from various noises.

V. CONCLUSION

In this letter, we propose a soft tactile sensor with two channels to obtain contact information. In our analysis, we arranged two channels filled by ionic gels, which are conductive materials, such that they were placed parallel from the top view and crossed from the side view. As the channel resistance is known to depend on the channel width, the shallower the channel, the greater the deformation, and the greater the resistance change. We hypothesized that the proposed sensor could estimate the contact position solely by calculating the resistance change ratio for the two channels, and the pressure could be calculated based on the theoretical equation using the estimated position. We observed that the proposed sensor could successfully estimate the contact position and pressure. Therefore, we concluded that the proposed sensor can classify the contact position and contact pressure. In future studies, we intend to improve the sensor sensitivity and develop further applications.

ACKNOWLEDGMENT

This work was supported by JSPS KAKENHI under Grant JP19H01122, Grant JP20K14696, Grant JP20K19820, and Grant JP23H00498. The authors would like to thank Prof. H. Furukawa, Dr. K. Yoshida at Yamagata University for useful comments and providing the ionic gels, Dr. S. Shigaki for technical advice, and Editage for English language editing.

REFERENCES

[1] S. Takamuku, A. Fukuda, and K. Hosoda, "Repetitive grasping with anthropomorphic skin-covered hand enables robust haptic recognition," in *Proc. IEEE/RSJ Int. Conf. Intell. Robots Syst.*, 2008, pp. 3212–3217.

[2] S. Funabashi et al., "Object recognition through active sensing using a multi-fingered robot hand with 3D tactile sensors," in *Proc. IEEE/RSJ Int. Conf. Intell. Robots Syst.*, 2018, pp. 2589–2595.

[3] L. E. Osborn et al., "Prosthesis with neuromorphic multilayered e-dermis perceives touch and pain," *Sci. Robot.*, vol. 3, no. 19, 2018, Art. no. eaat3818.

[4] S. Pirozzi and C. Natale, "Tactile-based manipulation of wires for switchgear assembly," *IEEE ASME. Trans. Mechatron.*, vol. 23, no. 6, pp. 2650–2661, Dec. 2018.

[5] Y. She, S. Wang, S. Dong, N. Sunil, A. Rodriguez, and E. Adelson, "Cable manipulation with a tactile-reactive gripper," *Int. J. Robot. Res.*, vol. 40, no. 12–14, pp. 1385–1401, 2021.

[6] M.-A. Lacasse, V. Duchaine, and C. Gosselin, "Characterization of the electrical resistance of carbon-black-filled silicone: Application to a flexible and stretchable robot skin," in *Proc. IEEE Int. Conf. Robot. Automat.*, 2010, pp. 4842–4848.

[7] W. W. Lee et al., "A neuro-inspired artificial peripheral nervous system for scalable electronic skins," *Sci. Robot.*, vol. 4, no. 32, 2019, Art. no. eaax2198.

[8] S. Muller, D. Seichter, and H.-M. Gross, "Cross-talk compensation in low-cost resistive pressure matrix sensors," in *Proc. IEEE Int. Conf. Mechatron.*, 2019, pp. 232–237.

[9] J. Chossat, H. Shin, Y. Park, and V. Duchaine, "Soft tactile skin using an embedded ionic liquid and tomographic imaging," *ASME J. Mechanisms Robot.*, vol. 7, no. 2, 2015, Art. no. 021008.

[10] K. S. Kumar, P. Y. Chen, and H. Ren, "A review of printable flexible and stretchable tactile sensors," *Research*, vol. 11, 2019, Art. no. 3018568.

[11] Y. Hara, K. Yoshida, A. Khosla, M. Kawakami, K. Hosoda, and H. Furukawa, "Very wide sensing range and hysteresis behaviors of tactile sensor developed by embedding soft ionic gels in soft silicone elastomers," *Electrochem. Soc. J. Solid State Sci. Technol.*, vol. 9, no. 6, 2020, Art. no. 061024.

[12] Y. L. Park, C. Majidi, R. Kramer, P. Berard, and R. Wood, "Hyperelastic pressure sensing with a liquid-embedded elastomer," *J. Micromechanics Microeng.*, vol. 20, 2010, Art. no. 125029.

[13] S. Y. Won, H. K. Kim, M. E. Kim, and K. S. Kim, "Two-point discrimination values vary depending on test site, sex and test modality in the orofacial region: A preliminary study," *J. Appl. Oral Sci.*, vol. 25, no. 4, pp. 427–435, 2017.